Electronic and formation energies for deep defects in narrow-gap semiconductors

W. Li and J. D. Patterson
Physics and Space Sciences Department, Florida Institute of Technology, Melbourne, Florida 32901-6988
(Received 18 September 1995; revised manuscript received 18 December 1995)

We consider the charged states of certain deep defects in the narrow-gap semiconductors mercury cadmium telluride, mercury zinc telluride, and mercury zinc selenide. We predict the values of the deep-defect energy levels and also the formation energy of the defects. For each charged state we include the effect of relaxation. We consider substitutional and interstitial anions and cations as well as vacancies. We use Green's-function techniques throughout and adapt the Haldane-Anderson model to consider the effects of different charged states. By use of a pseudopotential we generalize the ideal vacancy model so as to be able to consider relaxation. As always, chemical trends were predicted with considerably more accuracy than the absolute location of the energy levels. Formation energies, involving differences, were predicted with an accuracy similar to that of chemical trends. The more negatively charged the impurity, the higher the energy except that the vacancy energy did not depend strongly on the charge. Typical charge-state energy shifts of defect levels are about twice that caused by relaxation effects. Formation energies for defects in the same material and at the same site were quite similar while the formation energy for different charged states could vary considerably. If one considered only native defects, self-interstitials had the lowest formation energy while for antisites and vacancies the results were similar. [S0163-1829(96)05923-1]

I. INTRODUCTION

In a previous paper we used a Green's-function technique to calculate the position of certain deep defects in mercury cadmium telluride (MCT), mercury zinc telluride (MZT), and mercury zinc selenide (MZS).[1] Both substitutional and interstitial cation and anion site impurities were considered. The effect of lattice relaxation is important and was included. The prediction of the absolute position of the energy levels is very difficult but we expect (based on the results in previous papers, especially Ref. 1) that our precision was relatively good, and so chemical trends were accurately predicted. In this paper we look at the effect of various charged states on the location of the deep defect energies and also predict their formation energies. Finally we use pseudopotential ideas to predict formation energies and the location of the vacancy levels including the effects of relaxation.

The use of Green's-function techniques to calculate formation energies is new. The formation energies are calculated from the difference between the binding energy of the crystal with a ''perfect'' cluster and that with a defect cluster. That is, our calculation of formation energy is based on the difference between the binding energy of the crystal with and without the defects, where of course the self-energy of the defect therefore would not be included [see Eq. (4)]. This is an approximation, but similar ideas have been used to calculate defect formation energies.[2–4] We also realize that in a more accurate model the formation energy is a function of chemical potential,[5,6] however, in the case of narrow-gap semiconductors, we assume this variation is small.

In Sec. II we discuss our calculation methods using Green's functions; in Sec. III we give results for the energy levels for substitutional and interstitial deep defects; in Sec. IV we give results for formation energies of substitutional and interstitial deep defects; in Sec. V we give deep defect and formation energies for a modified vacancy model; and finally in Sec. VI we discuss our results and make our conclusions.

II. CALCULATIONAL METHODS USING GREEN'S FUNCTIONS

For our calculations, we start with the basic ideas of Hjalmarson *et al.*[7] We add the spin-orbit interaction for the II-VI materials, following the ideas of Kobayashi, Sankey, and Dow.[8] We also adapt the idea of Lee, Dow, and Sankey[9] for different charge states and follow Haldane and Anderson[10] to calculate their effects. In addition, we adapt the work of Li and Myles[11,12] to include relaxation effects. The deep energy levels associated with the neighborhood of the impurity are determined self-consistently. An sp^3s^* tight-binding model for electronic band structure with the narrow-gap semiconductors treated in the virtual crystal approximation was used.

The basic Green's-function calculation has already been completely discussed.[1] In what follows, we summarize the additional details needed for understanding the effects of different charge states and the special techniques used for calculating formation energies. All our calculations are for narrow-gap semiconductors.[13]

The charged-state splitting of a deep level in the band gap is the difference between the ionization energy of the ''nominal'' impurity and the ionization energy of the impurity in a charged state caused by the addition of electrons or holes. The ionization energy of an impurity in a semiconductor is defined as the energy required to remove an electron (or hole) from the occupied deep level to the conduction (or valence) band. In simplified one-electron theories, the defect potential may not include the interaction between electrons and hence be charged-state independent. To study charge-state splitting, the interactions must be included in some approximation.

We combine Hjalmarson's deep-level theory with

0163-1829/96/53(23)/15622(9)/$10.00 © 1996 The American Physical Society

Haldane and Anderson's model of Coulomb effects to study the charge-state splitting of the deep levels. The use of the Haldane and Anderson models enables us to include many-electron effects while retaining much of the simplicity of Hjalmarson's theory. This idea has been successfully utilized by Lee, Dow, and Sankey[9] to study charged-state splitting of deep levels in Si, by Sankey and Dow[14] to treat interstitials in Si, and by Myles[12] to treat substitutional impurities in MCT. The ideas used to evaluate charged-state splitting are fairly simple. The defect potential is assumed to depend on the parameter U_i where

$$U_i=\beta_i(E^i_{\text{imp}}-E^i_{\text{host}}), \quad (1)$$

where E^i_{imp} and E^i_{host} are, respectively, the defect and host atomic orbital energies for states of symmetry i, and the β_i are empirical parameters. The E^i_{imp} are evaluated by the Haldane-Anderson model.

A point defect in a tetrahedral site of a zinc-blende materials has point group T_d. A deep-level produced by such a defect can have either nondegenerate A_1 (s-like) symmetry or triply degenerate T_2 (p-like) symmetry. Since we are dealing with II-VI semiconductors spin-orbit coupling had to be included in the band-structure calculations that we used. However, in the part of the Hamiltonian that describes the defect, the effect of spin-orbit interaction is weak and can be neglected.[1] Thus for the defect, including spin only doubles the degeneracy of each level. Thus we have twofold degenerate A_1 levels and sixfold degenerate T_2 levels. We finally find, following the Haldane and Anderson approach,

$$U_{A_1}=\beta_{A_1}\{[E^0_s+U_{ss}n_{A_1}+6U_{sp}n_{T_2}]-E^{A_1}_{\text{host}}\}, \quad (2)$$

$$U_{T_2}=\beta_{T_2}\{[E^0_p+5U_{pp}n_{T_2}+2U_{sp}n_{A_1}]-E^{T_2}_{\text{host}}\}, \quad (3)$$

where the parameters E^0_s, E^0_p, U_{ss}, U_{sp}, and U_{pp} have been determined by Sankey and Dow[14] for the atoms that we consider. The quantities n_{A_1} and n_{T_2} are not necessarily integers because the atoms are embedded in a solid. They depend on the defect potential V and energy level E and can be evaluated in a standard way allowing for contributions from both the valence and deep levels.[9] Since they depend on E, solutions for the energy levels must be obtained by iteration. Similarly to the discussion in Sec. V the effects of lattice relaxation are also included in this calculation.

We next discuss the formation energy. In general, the defect concentration depends exponentially on and is primarily determined by the defect formation energy. The defect formation energy is the change in energy necessary to produce the defect and is computed approximately from[2]

$$E_f=E_b(\text{crystal with defect cluster})-E_b(\text{perfect crystal}), \quad (4)$$

where the first term in the difference is the total (negative) binding energy of the crystal with a defect cluster and the second term is the total (negative) binding energy of the crystal with a "perfect" cluster, i.e., a perfect crystal. In the Green's-function method the one-electron Schrödinger equation is transformed into a matrix equation with a size determined by the perturbing potential of the defect, which in turn is determined by the size of the defect cluster. Free atom parameters plus adjustment for the lattice define the diagonal part of the impurity potential. The off-diagonal part is defined by a constant determined by the host and the impurity and by the host interatomic distance as well as the distance d_1 between the impurity and its nearest neighbors. The distance d_1 in the relaxed state is determined by molecular dynamics.

Including second nearest neighbors, the clusters have a size, for zinc blende semiconductors, of 17 atoms including four nearest neighbors, and twelve next nearest neighbors. The total energy of the cluster is the sum of one-electron energies and the repulsion energy. The repulsion energy contains a correction for double counting introduced by summing over the one-electron energies. Again relaxation of neighbors and different charges are considered. The evaluation of the one-electron and repulsion energies is discussed later.

III. DEEP LEVELS FOR SUBSTITUTIONAL AND INTERSTITIAL DEFECTS

The electronic properties of deep levels can be studied with various degrees of sophistication. In all cases, we focus on chemical trends in the ordering of the deep levels. In Ref. 1 we consider the effects of lattice relaxation on the deep levels. In this paper, we further consider the effects of different charge states. Unless otherwise specified, we have standardized our calculation with a band gap of 0.1 eV. The corresponding x values are

$$x(\text{MCT}=\text{Hg}_{1-x}\text{Cd}_x\text{Te})=0.22,$$

$$x(\text{MZT}=\text{Hg}_{1-x}\text{Zn}_x\text{Te})=0.15,$$

$$x(\text{MZS}=\text{Hg}_{1-x}\text{Zn}_x\text{Se})=0.08.$$

Our impurities are surrounded by either cations (+) or anions (−). In their normal lattice positions in our compounds, the group II elements Hg and Cd become cations and the group VI elements Te and Se become anions. As far as lowering the potential energy goes, cation sites surrounded by negative ions tend to form s-like levels (because this keeps negative charges as well separated as possible). Anion sites surrounded by positive ions tend to form p levels that spread the negative charge out to the positive sites. Of course, covalent bonding and other effects can complicate this analysis. Presumably because they are often relatively compact, cation site s-like levels tend not to be affected appreciably by relaxation effects.

To understand our notation for charged states, consider the charged state of Zn when it substitutes for Te in MCT. Atomic zinc has a deficit of four electrons over atomic Te. We define Zn(n) (where n stands for "nominal") as Zn with two more electrons in the atomic state so it will be similar to the Te^{--}, which it replaces. Zn(n) will thus have two electrons in the $4s$ state and two in the $4p$ state. In the same notation Zn($n+$) has one $4p$ electron and Zn($n-$) will have three. Other impurities can be discussed in a similar manner.

We present our results in Figs. 1–3. In these figures we only consider anion site, p-like and cation site s-like levels since the deep levels in the other two possible cases are far from the energy gap (presumably, the s-like states on the

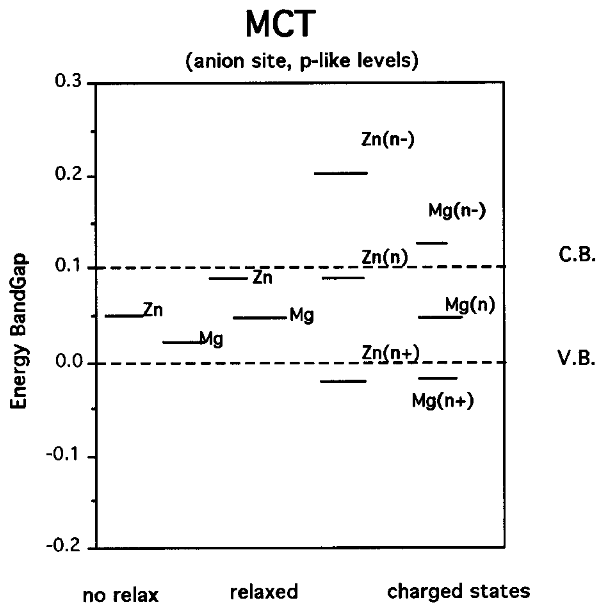

FIG. 1. Deep levels for substitutional impurities in MCT showing effects of relaxation and charged states (with relaxation).

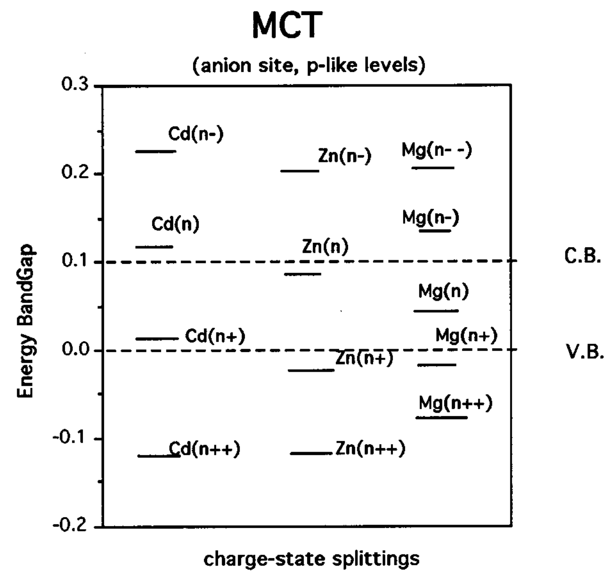

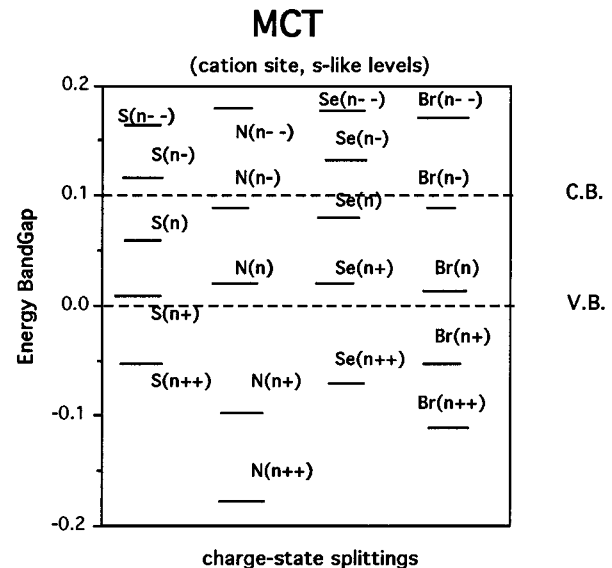

FIG. 2. Deep levels for charged states of substitutional defects: (a) anion site in MCT, (b) cation site in MCT, (c) anion site in MZT, (d) anion site in MZS.

anion are in the valence band, while the p-like states on the cation produce a resonance in the conduction band). In these figures, the bottom of the energy gap is at 0.0 eV and the top is at 0.1 eV. Figure 1 shows the effect of relaxation and different charged states for two impurities. As shown, charged-state interactions are typically about twice as important as relaxation effects. Figure 2 shows anion site p-like and cation site s-like levels in MCT and anion site, p-like levels in MZT and MZS. Our main objective has been to discuss chemical trends and generally we ignore the Jahn-Teller effect, which can be important in some cases. For example, the Zn^+ state of MZS in Fig. 2(d) is a triply degenerate state with a single $(4p)$ electron. Since this is Jahn-Teller unstable what we would probably see experimentally is a split-off singlet.

Some interesting observations can be made from these figures. In the first place, the negatively charged impurities form deep levels of higher energy than the nominal levels, which are in turn higher than the positively charged states. Coulomb repulsion between electrons provides a ready explanation for this. Second, the energy shift of the deep levels is a rough linear function of the charged state for a particular impurity. Thus, the energy shift for one more or one less electron in an impurity is about the same. For example, all the energy shifts in going from $Zn(n++)$ to $Zn(n+)$ to $Zn(n)$ to $Zn(n-)$ to $Zn(n--)$ are between 0.10 and 0.12 eV. Similar energy shifts in the Mg series range from 0.07 to 0.08 eV. That is, for different impurities, the energy shift between charged states for the same impurity should be close. Third, the chemical trends in the ordering of deep levels associated with different impurities for the same charged states are essentially unchanged. For example, $Zn(n)$ is above $Mg(n)$ in MCT, MZT, and MZS. Again we expect chemical trends to be much more accurate than absolute values. As noted by Chen and Sher,[15] the absolute location of the energy level may depend sensitively on the band structure and impurity potential.

Figure 3 summarizes the results for interstitial impurities in MCT, MZT, and MZS. Interstitial sites may have either hexagonal or tetrahedral symmetry. For interstitials, we only consider tetrahedral sites and name them in the same way as for substitutional ones, for example, cation sites are surrounded by negative ions. Five charged states are considered for each impurity of interest. In the case of interstitial impurities, the meaning of a nominal state is not the same as for a substitutional impurity. Here the number of electrons on a nominal state is the same as the number of valence electrons of the impurity in its atomic state. For example, the interstitial $Zn(n)$ in MCT has two electrons in the $3s$ states and no electrons in $4p$ states (rather than two in the $4p$ state as

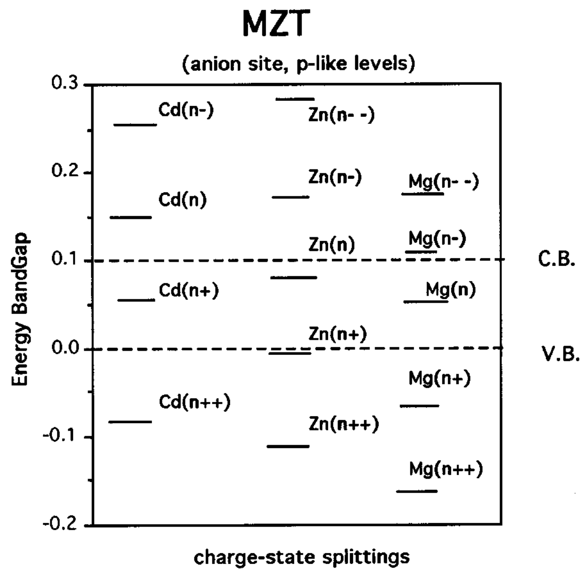

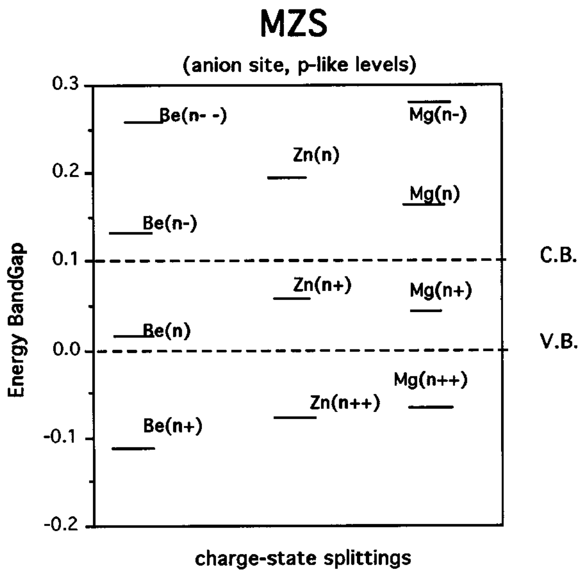

FIG. 2. (*Continued*).

when it substituted for Te in MCT), so here nominal does mean neutral. Similar discussion holds for other interstitial impurities.

Inspecting these figures, one sees that the deep levels formed by interstitial impurities with different charged states have similar properties to the substitutional cases. Again, the deep-level energy values are roughly a linear function of the charge, the negatively charged states have higher energy than neutral or positively charged levels, and the chemical trends of the ordering of the deep levels associated with different impurities for the same charged state are essentially preserved. However, charge-state splitting tends to be a little larger for interstitial impurities than substitutional ones. The neighboring ions are closer for the interstitial case.

The charged-state splitting as a function of alloy composition (x) has also been studied. Table I gives the results for

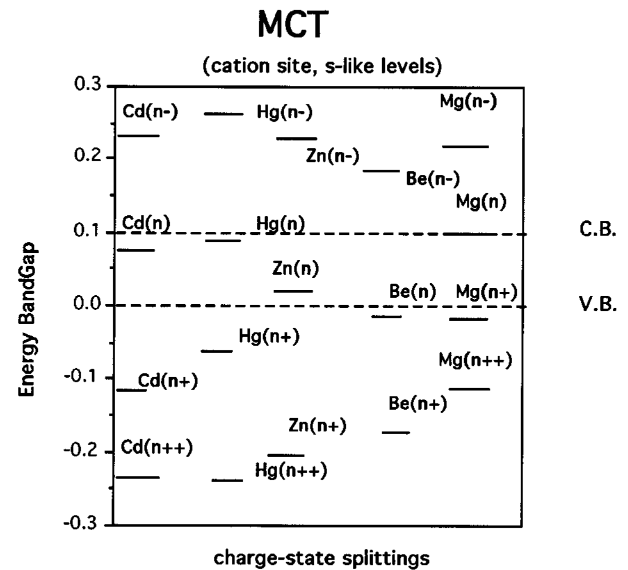

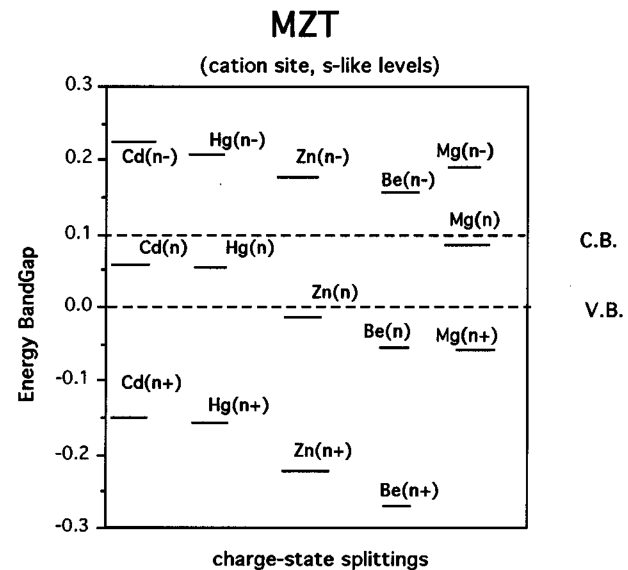

FIG. 3. Deep levels for charged states of interstitial impurities: (a) MCT, (b) MZT, and (c) MZS.

charged-state splitting of anion site, p-like deep levels for Zn and Mg in MCT for $x = 0.2$, 0.3, and 0.5. ΔE is the charged-state splitting. The splittings are of order 0.1 eV for different x and tend to vary only slightly with x. The results for three different degrees of sophistication of computation have been shown in Fig. 1 for the substitutional impurities Zn and Mg in MCT. As mentioned, one can see from the figure that the effects of charged-state splitting on deep levels are larger by about a factor of two than the effects of lattice relaxation. Our calculation shows this to be true for all defects of interest. In general, the effects of charge-state splitting can be comparable to the energy gap. Thus again we see the absolute location of the deep defect level is much more difficult to predict than chemical trends.

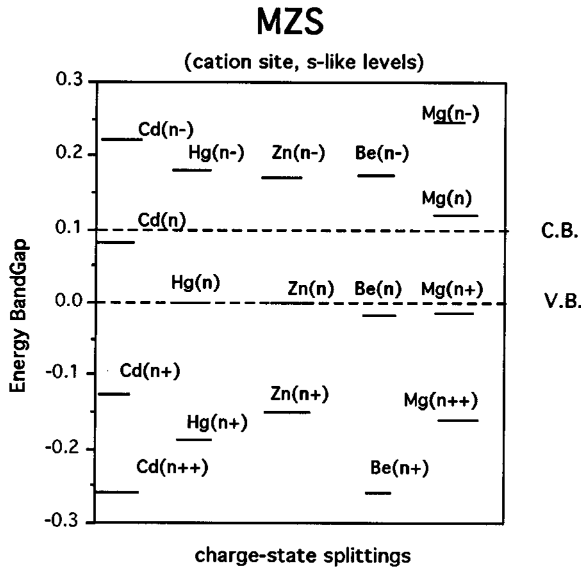

FIG. 3. (*Continued*).

IV. FORMATION ENERGY FOR SUBSTITUTIONAL AND INTERSTITIAL DEEP LEVELS

Our calculations borrow semiempirical band structure results and use Green's functions derived from these bands structures. The use of the tight-binding Green's function is certainly not new but the application of these Green's functions to the calculation of formation energies is new, to the best of our knowledge. Since the formation energy involves a difference of energies, it should have the same level of accuracy as the Green's function prediction of chemical trends for deep defect levels.

We continue to use the definition of the formation energy as the difference between the binding energy of the crystal with and without defects, as expressed by Eq. (4) and related[2] comments. The bonds at the cluster edges are coupled to the infinite host crystal. For the cluster without the defect, we keep the same values of tight-binding parameters as in the infinite host crystal. For the cluster with the defect, the defect potential matrix will be included. In this approach the surfacelike states associated with the cluster boundary are eliminated. This is the same idea as we have used to calculate the deep levels in our previous work.[1]

The total energy of a cluster with or without a defect can be modeled by

$$E^{\mathrm{tot}}=E^{\mathrm{el}}+E^{r}, \tag{5}$$

where E^{el} is the sum of the one-electron energies in the occupied states, and E^{r} is the repulsive energy due to electron-electron ion-ion repulsion and contains a correction for double counting contained in E^{el}. E^{el} can be computed as follows:

$$E^{\mathrm{el}}=\int_{-\infty}^{E_F} E\rho(E)dE, \tag{6}$$

where E_F is the Fermi energy and $\rho(E)$ is the electronic density of states given by

$$\rho(E)=-\frac{1}{\pi}\mathrm{Im}\ \mathrm{Tr}G(E), \tag{7}$$

where $G(E)$ is the Green's-function matrix. E^{r} can be computed using Harrison's[16] overlap interaction model for a pair potential in which

$$E^{r}=A'/d^{4}, \tag{8}$$

where A' is a proportionality constant, and d is the defect bond length. The constant A' can be determined from the equilibrium position of an atom in a perfect crystal. A detailed discussion has already been given by us and we summarize it below.[1] The total force on an atom due to the surrounding atoms in a certain direction can be modeled as

$$F_x=F_x^{a}+F_x^{r}, \tag{9}$$

where F_x^{a} and F_x^{r} represent the attractive and repulsive parts of the force. For the host crystal in the absence of the impurity, each atom is fixed in its equilibrium position for the perfect crystal so that $F_x=0$ and $F_x^{a}=-F_x^{r}$. Since $F_x^{r}=-\partial E^{r}/\partial x$, for x along the bond direction

TABLE I. Comparison of charge-state splittings for $x=0.2$, 0.3, and 0.5 in MCT.

	Deep levels (anion site, p-like)			ΔE		
Impurity	$x=0.2$	$x=0.3$	$x=0.5$	$x=0.2$	$x=0.3$	$x=0.5$
Zn($n--$)	$3.3E_g$	$3.3E_g$	$3.4E_g$	0.12	0.11	0.11
Zn($n-$)	$2.1E_g$	$2.2E_g$	$2.3E_g$	0.12	0.13	0.13
Zn(n)	$0.9E_g$	$0.9E_g$	$1.0E_g$			
Zn($n+$)	$-0.2E_g$	$-0.2E_g$	$-0.1E_g$	0.11	0.11	0.11
Zn($n++$)	$-1.2E_g$	$-1.1E_g$	$-1.0E_g$	0.10	0.09	0.09
Mg($n--$)	$2.1E_g$	$2.1E_g$	$2.2E_g$	0.08	0.08	0.09
Mg($n-$)	$1.3E_g$	$1.3E_g$	$1.3E_g$	0.08	0.08	0.07
Mg(n)	$0.5E_g$	$0.5E_g$	$0.6E_g$			
Mg($n+$)	$-0.2E_g$	$-0.2E_g$	$-0.1E_g$	0.07	0.07	0.07
Mg($n++$)	$-0.9E_g$	$-0.9E_g$	$-0.8E_g$	0.07	0.07	0.07

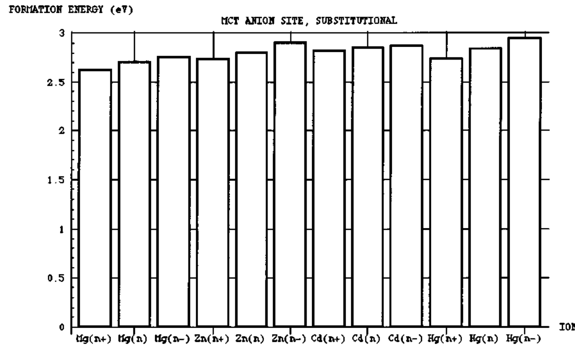

(a)

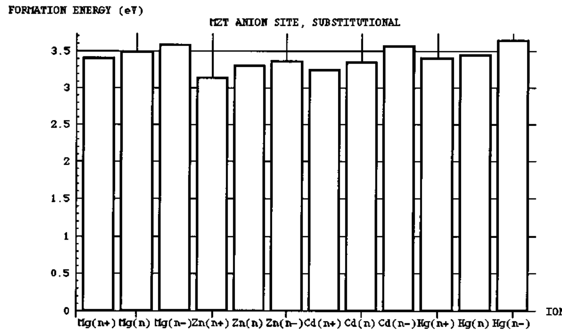

(b)

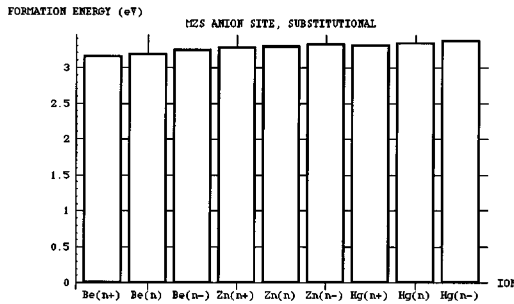

(c)

FIG. 4. Formation energies for charged states of anion site, p-like substitutional impurities: (a) MCT, (b) MZT, and (c) MZS.

$$F_x^r = \frac{4A'}{d^5}. \tag{10}$$

If we assume $F_x = A/d^5$ and use $F_x = 0$ in equilibrium to determine A, then $A' = A/4$. Admittedly, this procedure is somewhat arbitrary and certainly has not been justified rigorously. All we are really doing is fitting the force to an inverse fifth-order power law.

In Figs. 4 and 5 the formation energies of substitutional impurities in MCT, MZT, and MZS are evaluated. All anion site impurities are p-like and all cation sites are s-like. The same holds true in Fig. 6, where the formation energy of interstitial impurities in the same materials is considered. All results include relaxation. Several observations can be made for the substitutional case. The formation energies for the same material on the same site (cation or anion) can be quite similar. In MCT the formation energies of several nominal

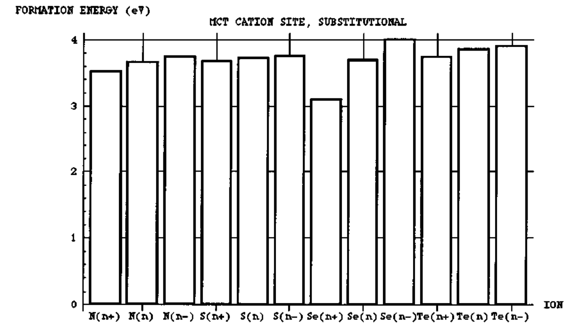

(a)

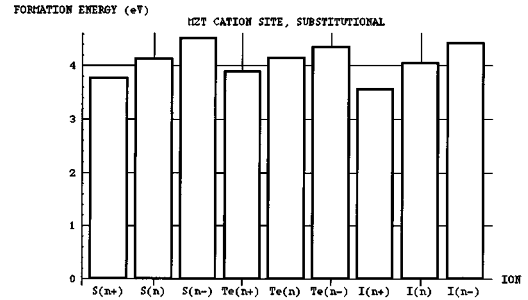

(b)

FIG. 5. Formation energies for charged states of cation site, s-like substitutional impurities: (a) MCT and (b) MZT.

impurities in eV are Zn(n) (2.8), Mg(n) (2.7), Cd(n) (2.85), and Hg(n) (2.84). The formation energy for different charged states of impurities can vary fairly widely. In MCT: Zn($n+$) (2.73), Zn($n-$) (2.9), and Cd($n+$) (2.82), Cd ($n-$) (2.87). We also notice that for a given impurity, the formation energy of a negative impurity is larger than a positive one. This is basically due to the repulsive force between electrons. For the formation energies of interstitials in Fig. 6 a similar discussion to that of substitutional impurities can be made. In addition the results tend to be more widely spread, presumably because of the closer neighbors.

V. FORMATION AND DEEP-LEVEL ENERGIES FOR VACANCIES

In a previous study of vacancies in MCT, MZT, and MZS we used the ideal vacancy model in which we assumed that the vacancy was formed by removing an atom from the crystal while leaving all other atoms in the same position. In the Green's-function method, this model is implemented by setting the atomic orbital energy of a vacancy equal to infinity. The deep levels formed in the ideal vacancy model can be easily calculated as the model does not require (or allow) the inclusion of lattice relaxation.

In this paper, we introduce a modified vacancy model that allows consideration of lattice distortion in an efficient and direct way. This is accomplished by changing the assumptions concerning the atomic orbital energy of a vacancy. Following Bernholc, Liparo, and Pantelides[17] and Baraff and Schluter[18] we assume the atomic orbital energy equals the negative of the bulk "atomic" pseudopotential of the removed host atom (instead of infinity). Bernholc, Liparo, and

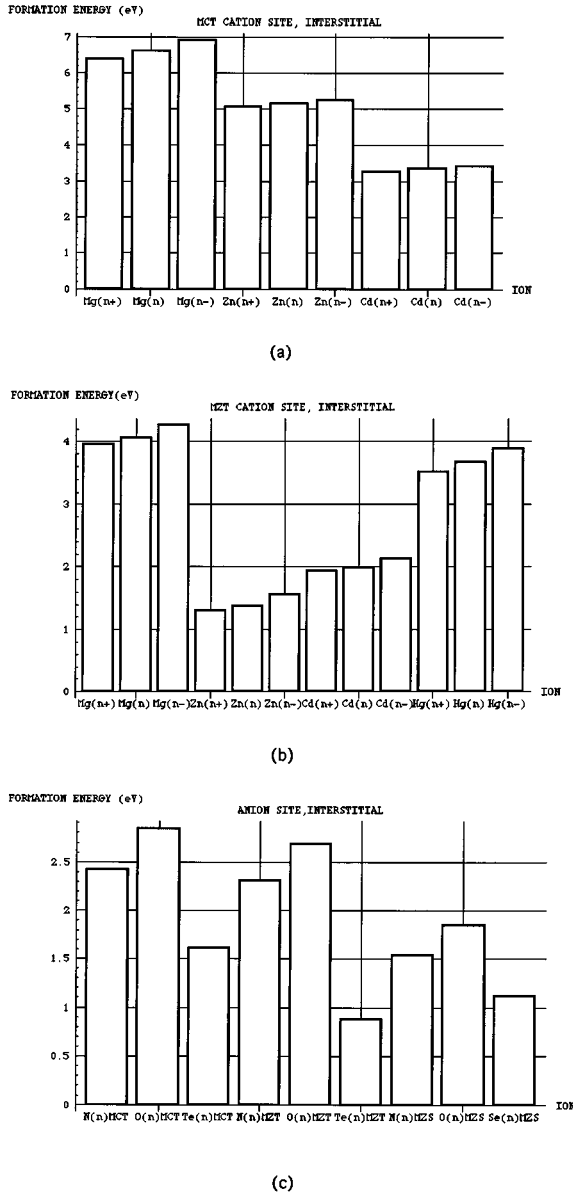

FIG. 6. Formation energies for several neutral and charged states of interstitial impurities: (a) cation site, s-like levels in MCT, (b) cation site, s-like levels in MZT, and (c) neutral anion site, p-like levels in several semiconductors.

Pantelides[17] have computed the defect potential of a vacancy in Si from this pseudopotential model. They found that the difference between results for a self-consistent model and the pseudopotential model was less than 1%.

Using the nearest-neighbor approximation, the form of the defect potential of a vacancy can be written as

$$V=\sum V_i=\sum |ia\mathbf{o}\rangle U^i_{aa}\langle ia\mathbf{o}|+\Sigma_{ij}|ia\mathrm{o}\rangle\alpha_i\langle jc\mathbf{d}|, \tag{11}$$

where $\mathbf{o}$ refers to the defect location, a and c refer to anion and cation sites, i and j refer to symmetric types (the A_1 and T_2 states), and $\mathbf{d}$ locates the neighbors.

In this form, the vacancy is at an anion site (a). The matrix form of V_i is thus

TABLE II. Lattice relaxation of vacancies in MCT, MZT, and MZS.

System	$d_H(A)$	$d_I(A)$	$\Delta x=d_I-d_H$	Percent of relaxation
MCT	2.8	3.02	0.22	7.6
MZT	2.74	2.45	−0.29	11.1
MZS	2.62	2.56	−0.06	2.3

$$V_i=\begin{bmatrix} U^i_{aa} & \alpha_i & \alpha_i & \alpha_i & \alpha_i \\ \alpha_i & & & & \\ \alpha_i & & & & \\ \alpha_i & & & & \\ \alpha_i & & & & \end{bmatrix}, \tag{12}$$

with

$$\alpha_i=-c_i(d_I^{-2}-d_H^{-2}), \tag{13}$$

where d_I is the distance between the center of the vacancy and the nearest neighbors and d_H is the distance between neighboring atoms in the perfect host crystal. In the ideal model U_{aa} is set to infinity and α is thus negligible. In the pseudopotential, U_{aa} is the quantity set equal to the negative of the bulk ''atomic'' pseudopotential of the removed host atom.

The bulk pseudopotential of an atom can be written[19]

$$U^{ps}(\mathbf{r})=\sum_G [S^S(\mathbf{G})U^S(\mathbf{G})+iS^A(\mathbf{G})U^A(\mathbf{G})]e^{i\mathbf{G}\cdot\mathbf{r}}, \tag{14}$$

where U^S and U^A are called symmetric and antisymmetric form factors and the S's (structure factors) can be found from

$$S^S(\mathbf{G})=\cos\mathbf{G}\cdot\mathbf{T}, \tag{15a}$$

$$S^A(\mathbf{G})=\sin\mathbf{G}\cdot\mathbf{T}, \tag{15b}$$

where $\mathbf{G}$ is the reciprocal lattice vector and $\mathbf{T}=a(\frac{1}{8},\frac{1}{8},\frac{1}{8})$ with a the length of a side of the unit cube. Examples of the evaluation of U^{ps} with empirical parameters for important $U^S(\mathbf{G}),U^A(\mathbf{G})$ are given by Li.[19] The pseudopotential is fairly slowly varying with $\mathbf{r}$ and we evaluate only for $\mathbf{r}=0$. Based on the pseudopotential model, we have computed the lattice distribution of vacancies in MCT, MZT, and MZS. The results are shown in Table II. Table III gives our result for the formation energy of vacancies in MCT, MZT, and MZS.

All vacancies are cation site, since no anion site deep-level vacancies have been predicted by us. We found very little dependence of formation energy on charged state for vacancies. Consequently, we only report results for the neutral case. If we focus on native defects (antisite, self-interstitial, and vacancy) we find the self-interstitials usually have the lowest formation energy while the formation energies for antisites and vacancies are almost the same. For

TABLE III. Formation energy of vacancies in MCT, MZT, and MZS. V_a denotes vacancy and HC denotes host crystal.

System	E^{el} (eV)	E^r (eV)	E^t (eV)	E^f (eV)
MCT				
HC	−12.19	2.21	−9.98	
V_a	−8.93	1.63	−7.30	2.68
MZT				
HC	−13.85	0.89	−12.96	
V_a	−10.53	1.39	−9.14	3.81
MZS				
HC	−12.3	3.18	−9.12	
V_a	−10.86	3.49	7.37	1.75

example, in the case of MZT at a cation site Zn(n) has a formation energy of 1.38 eV while antisite Te(n) is 4.14 eV and the vacancy is 3.81 eV.

Finally, for completeness we show in Table IV the deep levels we predict using the pseudopotential model for vacancies in MCT, MZT,and MZS, and compare them to results for the ideal vacancy model. Again, we only consider vacancies at the cation site. For MCT and MZT the pseudopotential results are higher. In MZS the results are the same for both models due to pinning. Lattice relaxation has been included in calculating the formation energy but not in calculating the levels, as its effect is usually small.

VI. DISCUSSION

We have considered the charged states of deep effects in the narrow-gap semiconductors MCT, MZT, and MZS. We have predicted the deep-defect energy levels and formation energies for charged states of substitutional, interstitial, and vacancy defects. We have included the effect of relaxation of neighbors. The use of a Green's function to calculate formation energies is new as in the use of the pseudopotential method to generalize the ideal vacancy model so relaxation can be considered. We expect that the chemical trends and formation energies were predicted more accurately than the absolute location of the energy levels. There is relatively little experimentation upon which to base this expectation. Comparison to experiment for the defect levels themselves has already been made.[1] We have not been able to find any

TABLE IV. Deep levels of vacancies in MCT, MZT, and MZS. Deep levels are measured from the maximum valence-band edge.

System	Deep levels (eV) Ideal model	Pseudopotential model
MCT	−0.32	−0.18
MZT	−0.34	−0.25
MZS	0.06	0.06

well-identified formation energies that allow unambiguous experimental comparison to our calculations. However, comparison to some results of Sher *et al.*[20] seems to indicate at least a qualitative correctness for our results.

Typical of our own results are the following. (a) The charge-state energy-level shifts of the defect levels were about twice as large as relaxation effects. (b) The more negatively charged the impurity the higher the energy because of Coulomb repulsion. (c) The energy shift of the deep substitutional levels is a rough linear function of the charge state for a particular impurity. (d) Chemical trends in the ordering of deep levels associated with different impurities for the same charged state are essentially unchanged. (e) Charge state splitting for interstitial impurities tends to be a little larger than for substitutional ones. (f) Charge-state splitting for substitutional impurities may be of order 0.1 eV and vary only slightly with alloy concentration x. (g) Formation energies for the same material on the same site can be quite similar. (h) The formation energies for different charged states can vary widely. (i) The formation energy for a negative impurity is larger than a positive one. (j) Defect and formation energies for vacancies are predicted not to be heavily dependent on the charged state. (k) Relaxation can appreciably affect the deep levels in vacancies. (l) For native defects, self-interstitials had the lowest formation energy while antisites and vacancies had similar formation energies.

ACKNOWLEDGMENTS

This work has been supported by NASA Marshall Space Flight Center, Grant Number No. NAG 8-1094. The authors particularly wish to thank Dr. S. L. Lehoczky and Sharon Cobb for their help and support.

[1] W. Li and J. D. Patterson, Phys. Rev. B **50**, 14 903 (1994).

[2] Pan Bicai and Xia Shangda, Phys. Rev. B **49**, 11 444 (1994).

[3] Yang Jinlong, Xiao Chuanyun, Xia Shangda, and Wang Kelin, Phys. Rev. B **46**, 13 709 (1992).

[4] M. A. Berding, A. Sher, and A. B. Chen, J. Appl. Phys. **68**, 5064 (1990).

[5] S. B. Zhang and John E. Northrup, Phys. Rev. Lett. **67**, 2339 (1991).

[6] Robert W. Janson and O. F. Sankey, Phys. Rev. B **39**, 3192 (1989).

[7] H. P. Hjalmarson, P. Vogl, D. J. Wolford, and J. D. Down, Phys. Rev. Lett. **44**, 810 (1980).

[8] A. Kobayashi, Otto F. Sankey, and John D. Dow, Phys. Rev. B **25**, 6367 (1982).

[9] S. Lee, John D. Dow, and Otto F. Sankey, Phys. Rev. B **31**, 3910 (1985). See also O. F. Sankey and J. D. Dow, *ibid.* **27**, 7641 (1983).

[10] F. D. M. Haldane and P. W. Anderson, Phys. Rev. B **13**, 2553 (1976).

[11] Weigang Li and Charles W. Myles, Phys. Rev. B **47**, 4281 (1993).

[12] Charles W. Myles, J. Vac. Sci. Technol. A **6**, 2675 (1988).

[13] J. D. Patterson, Condens. Matter News **3**, 4 (1994).

[14] O. F. Sankey and J. D. Dow, Phys. Rev. B **27**, 7641 (1983).

[15] A. B. Chen and A. Sher, Phys. Rev. B **31**, 6490 (1985).
[16] W. A. Harrison, Phys. Rev. B **27**, 3592 (1983).
[17] J. Bernholc, Nunzio U. Liparo, and Sokrates T. Pantelides, Phys. Rev. B **21**, 3545 (1980).
[18] G. A. Baraff and M. Schluter, Phys. Rev. B **21**, 5662 (1979).
[19] Ming-Fu Li, *Modern Semiconductor Quantum Physics* (World Scientific, Singapore, 1994), pp. 4–20.
[20] A. Sher, M. A. Berding, M. van Schilfgaarde, and A. B. Chen, Semicond. Sci. Technol. **5**, C59 (1991).